Original paper

WinGadclas, a Windows program for gadolinite-supergroup minerals

Fuat YAVUZ

Department of Geological Engineering, Istanbul Technical University, 34469 Maslak, Istanbul, Turkey; yavuz@itu.edu.tr

A Microsoft® Visual Basic software, WinGadclas, has been developed to calculate the chemical formulae of gadolinite supergroup minerals based on data obtained from wet-chemical and electron-microprobe analyses. WinGadclas currently evaluates 13 valid mineral species using the Commission on New Minerals, Nomenclature and Classification (CNMNC) of the International Mineralogical Association (IMA) nomenclature scheme for the gadolinite-supergroup minerals in the general chemical formula $A_2MQ_2T_2O_8\varphi_2$. The program recalculates and estimates the chemical formulae of gadolinite-supergroup species based on 10 oxygen atoms, with the 2 *T*, 2 *A*, and $T+Q = 4$ atoms per formula unit normalization options. Mineral formulae of the gadolinite-supergroup minerals are calculated based on the occupancy of *A*, *M*, *Q*, *T*, and *φ* sites, as well as the application of the dominant-valency and dominant-constituent rules. WinGadclas operates in four stages: (1) it estimates cation and anion contents provided by input chemical data; (2) it determines the dominant cation and anion at the *A*, M, *Q*, *T*, and *φ* sites; (3) it assigns the gadolinite-supergroup minerals to one of the four subgroups, including datolite, gadolinite, herderite, and drugmanite; and (4) it classifies the gadolinite-supergroup species into appropriate groups, such as gadolinite and herderite. WinGadclas allows users to: (1) enter up to 46 input variables for mineral-chemical analyses; (2) type and load multiple gadolinite-supergroup mineral compositions in the data entry section; (3) edit and load the Microsoft® Excel files used in calculating, classifying, and naming the gadolinite--supergroup minerals, and (4) store all the calculated parameters in the output of a Microsoft® Excel file for further data evaluation. The program is distributed as a self-extracting setup file for Windows 7 or later operating system, including the necessary support files used by the program, a help file, and representative sample data files.

Keywords: gadolinite supergroup; datolite subgroup; gadolinite subgroup; herderite subgroup; drugmanite subgroup; classification
Received: September 2, 2025; accepted: November 13, 2025; handling editor: V. Janoušek
The online version of this article (doi: 10.3190/jgeosci.404) contains supplementary electronic material.

1. Introduction

The gadolinite-supergroup minerals, approved by the Commission on New Minerals, Nomenclature and Classification (CNMNC) of the International Mineralogical Association (IMA), have monoclinic symmetry with a $P2_1/c$ space group and are composed of gadolinite (silicates) and herderite (phosphates and arsenates) groups, respectively. The gadolinite-supergroup minerals have a layered structure consisting of two distinct layers that run parallel to the (100) plane and alternate in the [100] direction, in which one layer consists of TO_4 and QO_4 tetrahedra, while the other contains both $AO_6\varphi_2$ polyhedra and $MO_4\varphi_2$ octahedra (Bačík et al. 2017). The general chemical formula of gadolinite-supergroup minerals can be expressed as $A_2MQ_2T_2O_8\varphi_2$, where the letters, except for O for oxygen, specify groups of atoms to be applied for the dominant ion (e.g., Ca, Y, Ce, Yb, Nd, and Pb for *A*, and OH, O, and F for *φ*) based on the occupancy of the *A, M, Q, T,* and *φ* sites with the application of the dominant-valency and dominant-constituent rules. Each site in the gadolinite supergroup is occupied by: *A* = Ca, REE (Y and lanthanides), actinides (e.g., U, Th), Pb, Mn^{2+}, Bi; *M* = Fe, □ (vacancy), Mg, Mn, Zn, Cu, Al; *Q* = B, Be, Li; *T* = Si, P, As, B, Be, S; and *φ* = O, OH, F (Bačík et al. 2017). The gadolinite-supergroup minerals consist of two groups based on the charge occupancy at the *T* site, including the gadolinite group (i.e., Si^{4+} at the *T* site) and the herderite group (i.e., P^{5+} or As^{5+} at the *T* site). The gadolinite group is divided into the gadolinite and datolite subgroups according to divalent and trivalent cations occupying the *A* site, respectively. In this respect, the *Q* site is dominantly occupied by B^{3+} in the datolite subgroup, whereas Be^{2+} is the dominant cation in the gadolinite subgroup. Similarly, the herderite group minerals consist of two subgroups: herderite and drugmanite in which the *Q* site is dominantly occupied by Be^{2+} and a vacancy, respectively. Minerals of the herderite subgroup are characterized by the dominant divalent cation (e.g., Ca^{2+}) at the *A* site, Be^{2+} at the *Q* site, and a vacancy at the *M* site. On the other hand, the drugmanite subgroup is defined by the dominance of divalent cations (e.g., Pb^{2+}) at the *A* site, a vacancy situation at the *Q* site, and the occupation of cations (e.g., Fe^{3+}) at the *M* site (Bačík et al. 2017).

Although various computer programs applicable to the calculation and classification of rock-forming silicates,

Tab. 1 A list of the IMA-approved species in the gadolinite-supergroup minerals (revised from Bačík et al. 2017)

Row	Species	Symbol	Formula	*A*	*M*	*Q*	*T*	O	*φ*	IMA status
	Gadolinite Group									
	Datolite Subgroup			A^{2+}		Q^{3+}				
1	Datolite	Dat	$CaB(SiO_4)(OH)$	Ca^{2+}	□	B_2	Si_2	O_8	$(OH)_2$	A
2	Homilite	Hom	$Ca_2Fe^{2+}B_2Si_2O_{10}$	Ca^{2+}	Fe^{2+}	B_2	Si_2	O_8	O_2	A
	Gadolinite Subgroup			A^{2+}		Q^{2+}				
3	Gadolinite-(Y)	Gad-Y	$Y_2Fe^{2+}Be_2O_2(SiO_4)_2$	Y_2	Fe^{2+}	Be_2	Si_2	O_8	O_2	A
4	Gadolinite-(Ce)	Gad-Ce	$Ce_2Fe^{2+}Be_2O_2(SiO_4)_2$	Ce_2	Fe^{2+}	Be_2	Si_2	O_8	O_2	A
5	Gadolinite-(Nd)	Gad-Nd	$Nd_2Fe^{2+}Be_2O_2(SiO_4)_2$	Nd_2	Fe^{2+}	Be_2	Si_2	O_8	O_2	A
6	Hingganite-(Y)	Hin-Y	$BeY(SiO_4)(OH)$	Y_2	□	Be_2	Si_2	O_8	$(OH)_2$	A
7	Hingganite-(Ce)	Hin-Ce	$BeCe(SiO_4)(OH)$	Ce_2	□	Be_2	Si_2	O_8	$(OH)_2$	A
8	Hingganite-(Yb)	Hin-Yb	$BeYb(SiO_4)(OH)$	Yb_2	□	Be_2	Si_2	O_8	$(OH)_2$	A
9	Hingganite-(Nd)	Hin-Nd	$Nd_2□Be_2Si_2O_8(OH)_2$	Nd_2	□	Be_2	Si_2	O_8	$(OH)_2$	A
	Herderite Group									
	Herderite Subgroup			A^{2+}		Q^{2+}				
10	Herderite	Hrd	$CaBe(PO_4)F$	Ca_2	□	Be_2	P_2	O_8	F_2	A
11	Hydroxylherderite	Hhd	$CaBe(PO_4)(OH)$	Ca_2	□	Be_2	P_2	O_8	$(OH)_2$	A
12	Bergslagite	Bgl	$CaBe(AsO_4)(OH)$	Ca_2	□	Be_2	As_2	O_8	$(OH)_2$	A
13	*Fluorbergslagite*	Fbgl	$CaBe(AsO_4)F$	Ca_2	□	Be_2	As_2	O_8	F_2	NA
	Drugmanite Subgroup			A^{2+}		□				
14	Drugmanite	Dru	$Pb_2Fe^{3+}(PO_4)(PO_3OH)(OH)_2$	Pb_2	Fe^{3+}	$□_2$	P_2	$O_7(OH)$	$(OH)_2$	A

A = Approved by the IMA; NA = Not approved by the IMA; □ = Vacancy.

ore-related minerals, as well as accessory minerals, have been developed over the past two decades (e.g., Yavuz 1999, 2003, 2013; Yavuz et al. 2014, 2015; Yavuz and Yıldırım 2018, 2020; Yavuz 2021; Yavuz and Yavuz 2022, 2023a, b, 2024; Janoušek et al. 2024; Yavuz 2024a, b, 2025a, b), those useful for the gadolinite-supergroup minerals, according to the current IMA report, have not yet appeared in the literature, possibly in part due to the lack of a classification system until the one published only recently by Bačík et al. (2017). Taking this situation into consideration, a computer program called WinGadclas has been developed using the Microsoft® Visual Basic programming language. It can be used to calculate the chemical formulae from up to 200 analyses obtained from both wet-chemical and electron-microprobe techniques. The program estimates and classifies mineral analyses of gadolinite-supergroup minerals on the basis of 10 oxygen atoms, with the 2 *T*, 2 *A* and $T+Q=4$ atoms per formula unit (apfu) normalization options selected from the pull-down menu of *Calculate Contents of Ions* in the *Start-up Screen* or *Data Entry Screen*. The calculation and classification procedures applied to gadolinite supergroup minerals by WinGadclas are carried out according to the currently accepted IMA nomenclature scheme (Bačík et al. 2017), with changes to the gadolinite subgroup nomenclature proposed by Atencio (2023), who discredited minasgeraisite-(Y) (i.e., IMA-CNMNC Proposal 23-F). Hence, the program does not classify this type of species (e.g., minasgeraisite-(Y)) with the statement "Not classified" in column 121 of the *Calculation Screen*. Additionally, the program considers hypothetical end members (e.g., *fluorbergslagite*) as well as *new root names* based on analytical data or real substitution trends for classifying the gadolinite supergroup. WinGadclas allows the user to display members of the gadolinite supergroup in several binary and ternary classification and compositional diagrams by using Golden Software's Grapher program from the pull-down menu of *Graph* in the *Calculation Screen*.

2. Gadolinite-supergroup minerals nomenclature

The gadolinite supergroup comprises phosphates, beryllophosphates, berylloarsenates, borosilicates, and beryllosilicates. Among these, beryllosilicates are the most prevalent in nature, making up the majority of the supergroup species, and they are classified within the gadolinite subgroup (Bačík et al. 2017; Vereshchagin et al. 2023). Being a monoclinic orthosilicate member of the gadolinite-supergroup minerals, gadolinite commonly occurs in beryllium- and REE (rare earth element)-bearing granites, Nb–Y–F-rich (niobium–yttrium–fluorine) pegmatites, alkaline rocks, alkaline pegmatites or syenite pegmatites associated with larvikites, some metamorphic rocks, REE-rich Alpine-type hydrothermal mineralization, and iron-oxide skarn deposits (Segalstad and Larsen 1978; Pezzotta et al. 1999; Škoda et al. 2018 and references therein; Allaz et al. 2020). Members of the gadolinite subgroup with a magmatic origin are often metamict due to high contents of actinides (e.g., U, Th) replacing

REEs, i.e. structural disorder induced by radiation damage (Paulmann et al. 2019).

Using the available data on the gadolinite supergroup species, consisting of the gadolinite and herderite groups, Bačík et al. (2017) proposed a nomenclature scheme for the members, which has been approved by the IMA–CNMNC (see Tab. 1). In this nomenclature scheme, the gadolinite supergroup minerals with the general chemical formula $A_2MQ_2T_2O_8\varphi_2$, belonging to silicates, phosphates and arsenates, are classified based on the occupancy of *A*, *M*, *Q*, *T*, and φ sites, as well as the application of the dominant-valency and dominant-constituent rules (Hatert and Burke 2008). The dominant-valency rule is considered for the occupancy of the *A* and *M* sites due to the trivalent (i.e., R^{3+}) and divalent (i.e., R^{2+}) cations, as well as vacancies (i.e., □) at the *M* site, and also for the *T* site, which hosts various tetravalent (i.e., R^{4+}) and pentavalent (i.e., R^{5+}) cations. In the structure of gadolinite-supergroup minerals, there are tetrahedral sites that regularly form alternating four- and eight-membered rings, such as *T* and *Q*. In this structure, each TO_4 tetrahedron is connected to three QO_4 tetrahedra and vice versa (Bačík et al. 2017). The charge at the *T* site varies from 4^+ (e.g., Si) to 5^+ (e.g., P or As) within the TO_4 tetrahedron, which hosts the dominant cations of silicon, phosphorus, and arsenic in silicates, phosphates, and arsenates, respectively. In contrast to drugmanite, which is unique due to the vacancy at the *Q* site in the drugmanite subgroup (King and Sengier-Roberts 1988), the QO_4 tetrahedra are generally occupied by B for the datolite subgroup and by Be for the gadolinite and herderite subgroups.

The *A* site in the structure of gadolinite-supergroup minerals exhibits the highest coordination number of eight and is characterized by distorted tetragonal antiprisms (Cámara et al. 2008). Although cations with ionic radii between 1.331 Å (Pb) and 0.976 Å (Lu) can occupy the *A* site in the gadolinite supergroup due to a higher coordination number, the most frequently observed cations at this site are Ca (1.132 Å), Y (1.024 Å), and Ce (1.129 Å), with trace amounts of Mn (0.955 Å) (Bačík et al. 2017; Hawthorne and Gagné 2024). The charge at the *A* site ranges from 2^+ (e.g., Ca) to 3^+ (e.g., Ce), with no indication of monovalent cations (e.g., Na) being present. However, theoretically, there are no restrictions regarding local site dimensions or bond-valence requirements that would prevent the presence of monovalent cations at the *A* site. The $AO_6\varphi_2$ polyhedra are situated in layers that are interposed between two tetrahedral layers, creating a network of irregular six-membered rings. These rings enclose the *M* site and share edges with the $AO_6\varphi_2$ polyhedra, while the $AO_6\varphi_2MO_4\varphi_2$ layer is flanked by eight-membered tetrahedral rings (Bačík et al. 2014, 2017).

In the current gadolinite-supergroup minerals nomenclature scheme, the charge at the *M* site varies from 0 (i.e., vacant site) to 3^+ and the *M* site is predominantly occupied by Fe^{2+}, as in gadolinites (e.g., gadolinite-(Y)) and homilite. However, other divalent cations with ionic radii close to Fe^{2+} (e.g., Mg, Mn, Co, Ni, Cu, and Zn, Ni) can occupy the *M* site (Foit et al. 1973; Ito and Hafner 1974). The *M* site is also occupied by trivalent cations, like Fe^{3+}, as in the case of drugmanite. Conversely, the *M* site in other members of the gadolinite supergroup – excluding gadolinites, homilite, and drugmanite – is vacant (e.g., hingganite-(Ce)) with the charge balanced by the protonation of two oxygens at the $\varphi5$ anion sites. The distorted $MO_4\varphi_2$ octahedra are bounded by four-membered rings of *T* and *Q* tetrahedra on either side of the $AO_6\varphi_2MO_4\varphi_2$ layer. The *M*-site cations are coordinated with pairs of O2, O4, and $\varphi5$ anions, as well as O2 and O4 linking the TO_4 and QO_4 tetrahedra in neighbouring layers. The gadolinite-supergroup minerals that contain five anion sites with totalling 10 anions per formula unit (apfu) are exclusively occupied by oxygen in the O2–4 sites, whereas the O1 site may bond with one hydrogen atom, as in the case of drugmanite. The $\varphi5$ site may contain oxygen (e.g., gadolinite (Nd)), hydroxyl (e.g., hingganite-(Yb)), and fluorine (e.g., herderite), resulting in the anion component of the gadolinite supergroup structure with 16–20 negative charges (Bačík et al. 2014).

In the gadolinite supergroup, groups are named according to the oldest members as well as the prevailing occupancy at the *T* site based on the dominant-valence rule (Hatert and Burke 2008). For example, minerals with dominant Si^{4+} at the *T* site belong to the gadolinite group, whereas minerals with dominant pentavalent (i.e., R^{5+}) cations (e.g., P, As) at the *T* site belong to the herderite group. While using the occupancy of the *Q* sites as a classification criterion is not recommended due to the difficulties in analysing Be and B, determining the occupancy and dominant charge of the *A* site is generally sufficient for classifying a mineral into a subgroup. Bačík et al. (2017) stated that if the *Q*-site occupancy cannot be analytically determined and the occupation and dominant charge of the *A* site are inadequate for subgroup classification, the *M*-site occupancy can also be utilized to correctly assign a mineral to its appropriate subgroup. In the datolite subgroup, the *A* site is primarily filled with divalent cations, while in the gadolinite subgroup, it is mainly occupied by trivalent cations. Similarly, the *Q* site is predominantly occupied by B^{3+} in the datolite subgroup and by Be^{2+} in the gadolinite subgroup.

The herderite subgroup is characterized by the prevalence of divalent cations, typically Ca^{2+}, at the *A* site and Be^{2+} at the *Q* site. In contrast, the drugmanite subgroup is distinguished by the dominance of divalent cations, usually Pb^{2+}, at the *A* site, along with a vacancy at the *Q* site. The root name of gadolinite supergroup miner-

Tab. 2 Description of column numbers in the Calculation Screen window of WinGadclas program and an output Excel file

Row	Explanations	Column Numbers
1	Major oxides from the gadolinite-supergroup mineral (GSM) compositions (wt. %)	1–48
2	Blank	49
3	Estimation of the stoichiometric BeO, B_2O_3 and H_2O content (wt. %)	50–52
4	Blank	53
5	Recalculated cations from the GSM compositions (*apfu*)	54–98
6	Blank	99
7	Recalculated OH, O and F contents from the GSM compositions (*apfu*)	100–103
8	Blank	104
9	Total cations at the *A* site (*apfu*)	105
10	Total cations at the *M* site (*apfu*)	106
11	Total cations at the (*Q*+*T*) sites (*apfu*)	107
12	Ca/(Total *A* site) ratio	108
13	Si/(Total *T* site) ratio	109
14	Y/(Total *A* site) ratio	110
15	Total (REE+Y) contents (*apfu*)	111
16	Blank	112
17	Dominant ions at the sites (i.e., *A*, *M*, *Q*, *T*, and ϕ)	113–117
18	Blank	118
19	Group name, subgroup name, and species from the GSM compositions	119–121
20	Additional information about the GSM	122
21	Blank	123

(*apfu*) = Atoms per formula unit

als is determined based on the occupancy of the *A*, *M*, and *T* sites. In terms of the occupancy of the *A* site, for example, if the dominant cation at the *A* site in a new mineral is not a rare earth element, it is assigned a new root name. For instance, a mineral (e.g., homilite) with strontium as the dominant cation at the *A* site is not defined as homilite-(Sr) or strontio-homilite; instead, it is given a distinct root name. Similarly, if a newly identified ^{A}REE-dominant mineral varies from known species solely in its dominant REE, the Levinson-type suffix (Levinson 1966) is considered by appending the dominant REE to the existing root name. For example, Yb-dominant gadolinite is designated as gadolinite-(Yb) in the current gadolinite supergroup nomenclature scheme proposed by Bačík et al. (2017).

In the gadolinite-supergroup minerals, when the *M* site is occupied for homilite, gadolinites, or drugmanite, the predominant cation is typically Fe^{2+} or Fe^{3+}, as in the case of drugmanite. To date, no other cation has been reported to dominate the *M* site. If the occupancy of the *M* site exceeds 0.5 (apfu) and Fe^{2+} or Fe^{3+} is not the dominant cation, a new root name is used to define the gadolinite supergroup species. When the *T*-site population is changed through heterovalent substitution, a new root name is required due to the change in group classification. In contrast, homovalent substitution – such as replacing P with As – does not change the group name, but it is still advisable to assign a new mineral root name rather than rely on a prefix. Therefore, if a phosphate analogue of drugmanite exists, a new root name is used instead of the term *phosphodrugmanite* (Bačík et al. 2017). In the current gadolinite supergroup classification scheme, only a hydroxyl prefix (e.g., hydroxylherderite) is used to designate an occupant of the φ5 site.

In checking the literature, there are several possible procedures for calculating the chemical formulae of gadolinite-supergroup minerals. If all chemical data are available for a gadolinite supergroup mineral analysis, the calculation based on 10 anions is a proper method. In some instances, calculations involving anions are fundamentally flawed due to the presence of OH groups, the varying amounts of Fe^{3+}, and the levels of Be, B, and Li, which cannot be accurately measured by EMPA. Thus, if only EMPA data are available, a calculation procedure based on cations is a suitable approach. On the other hand, using a calculation based on five cations is fundamentally inappropriate due to the presence of a vacancy at the *M* site. Three other options for the calculation of the gadolinite supergroup minerals include (i) 4 (*A*+*T*), (ii) 2 *A*, and (iii) 2 *T* cations, respectively. Calculating based on 4 (*A*+*T*) cations is not recommended by Bačík et al. (2017) due to the potential for substitutions such as $CaFe_{-1}$, BSi_{-1}, or $AlSi_{-1}$. Likewise, replacing Si with B or Be at the *T* sites could also lead to a specific non-stoichiometric situation when the formula is based on 4 (*A*+*T*) or 2 *T* cations. In this instance, calculating based on 2 *A* cations may yield the correct formula. According to Bačík et al. (2017), in the absence of BSi_{-1} substitution, which is common in most of the gadolinite-supergroup minerals, it is advisable to calculate the formulae based on 2 *T* and 2 *A* cations at the same time and then select the formula that is more stoichiometrically appropriate, giving preference to the calculation based on the 2 *T* cations.

3. Program description

WinGadclas is a user-friendly, compiled program package (≈9 MB) developed for personal computers running on

the Microsoft® Windows operating system. The program first calculates the cation and anion values (in apfu) from analyses made on the gadolinite supergroup by means of wet-chemical or electron-microprobe techniques and then uses these to classify the mineral into the IMA-approved species that belong to two groups, i.e. gadolinite and herderite, with four subgroups consisting of datolite, gadolinite, herderite, and drugmanite (see Tab. 1). A list of the calculation steps in the *Calculation Screen* and in the output of a Microsoft Excel file developed by the program is given in Tab. 2. Upon the successful installation of WinGadclas, the start-up screen with various pull-down menus and equivalent shortcuts appears on the display (Fig. 1a). The program allows the user to input wet-chemical or electron-microprobe gadolinite supergroup analytical data by clicking the *New* icon on the toolbar, by selecting the *New File* from the pull-down menu of the *File* option, or pressing the *Ctrl+N* keys (Fig. 1b). Up to 46 chemical analytes (in wt. %) are used by WinGadclas given in the following order:

Sample No, SiO_2, TiO_2, ZrO_2, UO_2, ThO_2, Al_2O_3, Cr_2O_3, B_2O_3, Fe_2O_3, Y_2O_3, Bi_2O_3, La_2O_3, Ce_2O_3, Pr_2O_3, Nd_2O_3, Sm_2O_3, Eu_2O_3, Gd_2O_3, Tb_2O_3, Dy_2O_3, Ho_2O_3, Er_2O_3, Tm_2O_3, Yb_2O_3, Lu_2O_3, Nb_2O_5, Ta_2O_5, As_2O_5, Sb_2O_5, P_2O_5, FeO, MnO, CaO, BaO, SrO, MgO, NiO, ZnO, PbO, CuO, BeO, Na_2O, K_2O, LiO_2, F, H_2O.

Data from the analysis of a gadolinite-supergroup mineral can also be input into a blank Excel file following the above order, saving it with the extension of ".xls" or ".xlsx". After this, the file can be loaded into the *Data Entry Screen* of the program by clicking the *Open Excel File* option from the pull-down menu of *File*. By selecting the *Edit Excel File* option from the pull-down menu of *File*, data can be inserted into a blank Excel file (i.e., MyGadolinite), saved using a different file name (with the extension of ".xls" or ".xlsx"), and then loaded into the *Data Entry Screen* of the program by clicking the *Open Excel File* option from the pull-down menu of *File*. Additional information about data entry or similar topics can be accessed by pressing the F1 function key to display the WinGadclas.chm help file on the screen. The current version of WinGadclas includes a total of 17 binary and ternary classification and compositional plots. Data on any of these plots can be displayed using the program Grapher by selecting the diagram type from the pull-down menu of *Graph* in the *Calculation Screen* of the program (Fig. 1c).

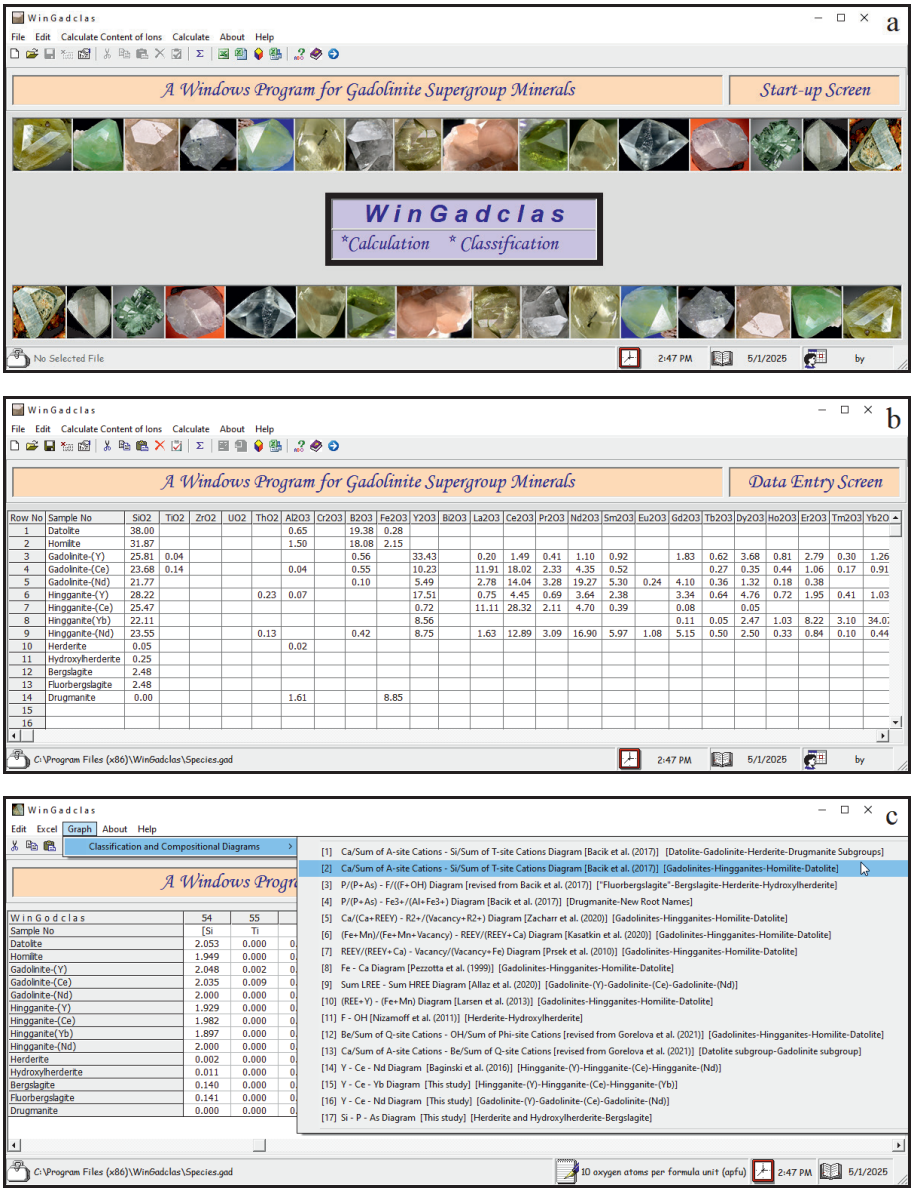

Fig. 1a – A screenshot of the WinGadclas Start-up window with various pull-down menus and equivalent shortcuts. **b** – A screenshot of the WinGadclas *Data Entry* window with a total of 46 analytes (wt. %). **c** – A screenshot of the WinGadclas *Calculation Screen* with plot options from the pull-down menu of the *Graph*.

Tab. 3 Chemical compositions of selected gadolinite group minerals with calculations and classifications by WinGadclas

Row		S1	S2	S3	S4	S5	S6	S7	S8	S9
1	SiO_2	38.000	31.870	25.810	23.680	21.770	28.220	25.470	22.110	23.550
2	TiO_2	0.000	0.000	0.040	0.140	0.000	0.000	0.000	0.000	0.000
3	ThO_2	0.000	0.000	0.000	0.000	0.000	0.230	0.000	0.000	0.130
4	Al_2O_3	0.650	1.500	0.000	0.040	0.000	0.070	0.000	0.000	0.000
5	B_2O_3	19.380	18.080	0.560	0.550	0.100	0.000	0.000	0.000	0.420
6	Fe_2O_3	0.280	2.150	0.000	0.000	0.000	0.000	0.000	0.000	0.000
7	Y_2O_3	0.000	0.000	33.430	10.230	5.490	17.510	0.720	8.560	8.750
8	La_2O_3	0.000	0.000	0.200	11.910	2.780	0.750	11.110	0.000	1.630
9	Ce_2O_2	0.000	0.000	1.490	18.020	14.040	4.450	28.320	0.000	12.890
10	Pr_2O_2	0.000	0.000	0.410	2.330	3.280	0.690	2.110	0.000	3.090
11	Nd_2O_3	0.000	0.000	1.100	4.350	19.270	3.640	4.700	0.000	16.900
12	Sm_2O_3	0.000	0.000	0.920	0.520	5.300	2.380	0.390	0.000	5.970
13	Eu_2O_2	0.000	0.000	0.000	0.000	0.240	0.000	0.000	0.000	1.080
14	Gd_2O_3	0.000	0.000	1.830	0.000	4.100	3.340	0.080	0.110	5.150
15	Tb_2O_3	0.000	0.000	0.620	0.270	0.360	0.640	0.000	0.050	0.500
16	Dy_2O_3	0.000	0.000	3.680	0.350	1.320	4.760	0.050	2.470	2.500
17	Ho_2O_3	0.000	0.000	0.810	0.440	0.180	0.720	0.000	1.030	0.330
18	Er_2O_3	0.000	0.000	2.790	1.060	0.380	1.950	0.000	8.220	0.840
19	Tm_2O_3	0.000	0.000	0.300	0.170	0.000	0.410	0.000	3.100	0.100
20	Yb_2O_3	0.000	0.000	1.260	0.910	0.000	1.030	0.000	34.070	0.440
21	Lu_2O_3	0.000	0.000	0.000	0.050	0.000	0.000	0.000	4.500	0.040
22	Nb_2O_5	0.000	0.000	0.270	0.000	0.000	0.000	0.000	0.000	0.000
23	FeO	0.000	16.250	12.350	10.110	10.620	4.370	3.610	0.000	3.030
24	MnO	0.390	0.000	0.110	1.280	0.100	0.230	0.000	0.000	0.100
25	CaO	35.390	27.280	0.900	3.130	0.140	4.370	7.070	1.140	0.450
26	MgO	0.090	0.520	0.000	0.320	0.510	0.000	0.000	0.000	0.000
27	ZnO	0.000	0.000	0.070	0.000	0.000	0.000	0.000	0.000	0.000
28	BeO	0.000	0.000	10.750	8.830	8.990	11.750	10.600	10.900	9.640
29	Na_2O	0.000	1.500	0.000	0.110	0.000	0.000	0.000	0.000	0.000
30	K_2O	0.000	0.000	0.000	0.540	0.000	0.000	0.000	0.000	0.000
31	H_2O	5.710	0.000	0.300	0.000	0.550	0.000	2.880	3.740	2.720
32	∑ (wt. %)	99.890	99.150	100.000	99.340	99.520	91.510	97.110	100.000	100.250
33	$B_2O_{3\ calculated}$ (wt. %)	0.000	0.000	0.000	0.000	0.000	2.710	2.190	0.000	0.000
34	$H_2O_{\ calculated}$ (wt. %)	0.000	0.850	0.000	0.660	0.000	5.780	0.000	0.000	0.000

4. Worked examples

Using the selected data set from the literature as well as "`Species.gad`" file in the installation document (i.e., WinGadclas setup file), examples are presented that show how WinGadclas can be used in the determination of chemical formulae and the classification of gadolinite-supergroup minerals. The previously typed or loaded analyses are processed by clicking the *Calculate* icon (i.e., ∑) in the *Data Entry Screen* of the program, after which all input and estimation parameters are displayed in columns 1–121 (see Tab. 2) of the *Calculation Screen*. Pressing the Ctrl+F keys or clicking the *Open File to Calculate* option from the *Calculate* menu also executes the processing of a selected data file with the extension of "`.gad`", which refers to the gadolinite supergroup. By clicking the *Send results to Excel file* icon in the *Calculation Screen*, all calculations can be stored in an Excel file (Output.xlsx) and then displayed by clicking the *Open and edit Excel file* icon.

The validity of program output has been tested with representative gadolinite group (see references in Tab. 3) and herderite group (see references in Tab. 4) analyses selected from the literature. WinGadclas calculates the compositional formula for a given gadolinite supergroup analysis on the basis of 10 oxygen atoms (*apfu*). Alternatively, by clicking one of the options, for example, *Based on the 2 T (apfu) Normalization* from the pull-down menu of *Calculate Contents of Ions* in the *Start-up Screen* or *Data Entry Screen*, the program calculates gadolinite-supergroup minerals according to the selected criteria. All input and calculated parameters are presented in the *Calculation Screen* and Excel output file for the selected mineral analyses from the literature. Classification of a given analysis into its proper group and subgroup is carried out based on the prevailing occupancy at the *T*

Tab. 3 Continued

Row		S1	S2	S3	S4	S5	S6	S7	S8	S9
35	Si	2.053	1.949	2.048	2.035	2.000	1.929	1.982	1.897	2.000
36	Ti	0.000	0.000	0.002	0.009	0.000	0.000	0.000	0.000	0.000
37	Th	0.000	0.000	0.000	0.000	0.000	0.004	0.000	0.000	0.003
38	Al	0.041	0.108	0.000	0.004	0.000	0.006	0.000	0.000	0.000
39	B	1.807	1.909	0.077	0.082	0.016	0.320	0.295	0.052	0.062
40	Fe^{3+}	0.011	0.099	0.000	0.000	0.000	0.000	0.000	0.000	0.000
41	Y	0.000	0.000	1.412	0.468	0.268	0.637	0.030	0.391	0.395
42	La	0.000	0.000	0.006	0.378	0.094	0.019	0.319	0.000	0.051
43	Ce	0.000	0.000	0.043	0.567	0.472	0.111	0.807	0.000	0.401
44	Pr	0.000	0.000	0.012	0.073	0.110	0.017	0.060	0.000	0.096
45	Nd	0.000	0.000	0.031	0.134	0.632	0.089	0.131	0.000	0.513
46	Sm	0.000	0.000	0.025	0.015	0.168	0.056	0.010	0.000	0.175
47	Eu	0.000	0.000	0.000	0.000	0.008	0.000	0.000	0.000	0.031
48	Gd	0.000	0.000	0.048	0.000	0.125	0.076	0.002	0.003	0.145
49	Tb	0.000	0.000	0.016	0.008	0.011	0.014	0.000	0.001	0.014
50	Dy	0.000	0.000	0.094	0.010	0.039	0.105	0.001	0.068	0.068
51	Ho	0.000	0.000	0.020	0.012	0.005	0.016	0.000	0.028	0.009
52	Er	0.000	0.000	0.070	0.029	0.011	0.042	0.000	0.222	0.022
53	Tm	0.000	0.000	0.007	0.005	0.000	0.009	0.000	0.083	0.003
54	Yb	0.000	0.000	0.030	0.024	0.000	0.021	0.000	0.891	0.011
55	Lu	0.000	0.000	0.000	0.001	0.000	0.000	0.000	0.117	0.001
56	Nb	0.000	0.000	0.010	0.000	0.000	0.000	0.000	0.000	0.000
57	Fe^{2+}	0.000	0.831	0.820	0.727	0.816	0.250	0.235	0.000	0.215
58	Mn	0.018	0.000	0.007	0.093	0.008	0.013	0.000	0.000	0.007
59	Ca	2.049	1.788	0.077	0.288	0.014	0.320	0.590	0.105	0.041
60	Mg	0.007	0.047	0.000	0.041	0.070	0.000	0.000	0.000	0.000
61	Zn	0.000	0.000	0.004	0.000	0.000	0.000	0.000	0.000	0.000
62	Be	0.000	0.000	2.049	1.823	1.984	1.929	1.982	2.247	1.967
63	Na	0.000	0.178	0.000	0.018	0.000	0.000	0.000	0.000	0.000
64	K	0.000	0.000	0.000	0.059	0.000	0.000	0.000	0.000	0.000
65	∑ (*apfu*)	5.988	6.909	6.909	6.902	6.851	5.982	6.443	6.105	6.229
66	OH	2.000	0.347	0.159	0.378	0.337	2.000	1.495	2.000	1.541
67	O	0.000	1.653	1.841	1.622	1.663	0.000	0.505	0.000	0.459
68	∑ (*apfu*)	2.000	2.000	2.000	2.000	2.000	2.000	2.000	2.000	2.000
69	∑ *A* site (*apfu*)	2.049	1.965	1.892	2.088	1.957	1.535	1.949	1.909	1.979
70	∑ *M* site (*apfu*)	0.078	1.086	0.834	0.874	0.894	0.269	0.235	0.000	0.222
71	∑ (*Q*+*T*) sites (*apfu*)	3.861	3.858	4.184	3.940	4.000	4.178	4.259	4.196	4.028
72	∑ (REE+Y) (*apfu*)	0.000	0.000	1.815	1.722	1.943	1.212	1.360	1.804	1.935
73	Ca/∑ A site	1.000	0.910	0.040	0.138	0.007	0.208	0.302	0.055	0.021
74	Si/∑ *T* site	0.532	0.505	0.490	0.517	0.500	0.462	0.465	0.452	0.496
75	Y/∑ *A* site	0.000	0.000	0.778	0.272	0.138	0.526	0.022	0.217	0.204
76	Dominant *A* site	Ca	Ca	Y	Ce	Nd	Y	Ce	Yb	Nd
77	Dominant *M* site	□	Fe^{2+}	Fe^{2+}	Fe^{2+}	Fe^{2+}	□	□	□	□
78	Dominant *Q* site	B	B	Be	Be	Be	Be	Be	Be	Be
79	Dominant *T* site	Si	Si	Si	Si	Si	Si	Si	Si	Si
80	Dominant *φ* site	OH	O	O	O	O	OH	OH	OH	OH
81	Subgroup	DatSg	DatSg	GadSg	GadSg	GadSg	GadSg	GadSg	GadSg	GadSg
82	Group	GadG	GadG	GadG	GadG	GadG	GadG	GadG	GadG	GadG
83	Species	Dat	Hom	Gad-Y	Gad-Ce	Gad-Nd	Hin-Y	Hin-Ce	Hin-Yb	Hin-Nd

Note: (*apfu*) = Atoms per formula unit. REEY = Rare Earth Elements + Y. □ = vacancy. Data sources: S1, S2 = Handbook of Mineralogy (Anthony et al. 2001–2005); S3, S6 = Lyalina et al. (2014); S4 = Segalstad and Larsen (1978); S5 = Škoda et al. (2018); S7 = Miyawaki et al. (2007); S8 = Voloshin et al. (1984); S9 = Kasatkin et al. (2020). GadG = Gadolinite group; DatSg = Datolite subgroup; GadSg = Gadolinite subgroup; Dat = Datolite, Hom = Homilite, Gad-Y = Gadolinite-(Y), Gad-Ce = Gadolinite-(Ce), Gad-Nd= Gadolinite-(Gd), Hin-Y = Hingganite-(Y), Hin-Ce = Hingganite-(Ce), Hin-Yb = Hingganite-(Yb), Hin-Nd = Hingganite-(Nd). The formulae were recalculated to *apfu* on the basis of 10 oxygens

Tab. 4 Chemical compositions of selected herderite group minerals with calculations and classifications by WinGadclas

Row		S1	S2	S3	S4	S5
1	SiO_2	0.050	0.250	2.480	2.480	0.000
2	Al_2O_3	0.020	0.000	0.000	0.000	1.610
3	Fe_2O_3	0.000	0.000	0.000	0.000	8.850
4	As_2O_5	0.000	0.000	51.580	51.580	0.000
5	P_2O_5	43.160	44.120	0.000	0.000	20.370
6	FeO	0.010	0.000	0.000	0.000	0.000
7	CaO	34.450	35.370	28.570	28.570	0.000
8	PbO	0.000	0.000	0.000	0.000	64.370
9	BeO	15.300	15.660	13.000	13.000	0.000
10	Na_2O	0.290	0.000	0.000	0.000	0.000
11	F	8.700	2.950	0.000	6.000	0.000
12	O=F	3.663	1.242	0.000	2.527	0.000
13	H_2O	1.390	4.240	6.000	0.000	3.870
14	∑ (wt.%)	99.707	101.348	101.630	99.103	99.070
15	$H_2O_{calculated}$ (wt.%)	0.000	0.000	0.000	0.900	0.000
16	[Si	0.002	0.012	0.140	0.153	0.000
17	Al	0.001	0.000	0.000	0.000	0.183
18	Fe^{3+}	0.000	0.000	0.000	0.000	0.644
19	As	0.000	0.000	1.522	1.662	0.000
20	P	1.763	1.735	0.000	0.000	1.667
21	Fe^{2+}	0.001	0.000	0.000	0.000	0.000
22	Ca	1.781	1.760	1.728	1.886	0.000
23	Pb	0.000	0.000	0.000	0.000	1.675
24	Be	1.773	1.747	1.762	1.924	0.000
25	Na	0.027	0.000	0.000	0.000	0.000
26	∑ (*apfu*)	5.349	5.254	5.152	5.625	4.170
27	OH	0.447	1.314	2.000	0.320	2.000
28	O	0.225	0.253	0.000	0.511	0.000
29	F	1.328	0.433	0.000	1.169	0.000
30	∑ (*apfu*)	2.000	2.000	2.000	2.000	2.000
31	∑ *A* site	1.808	1.760	1.728	1.886	1.675
32	∑ *M* site	0.002	0.000	0.000	0.000	0.827
33	∑ (*Q*+*T*) sites	3.539	3.494	3.424	3.738	1.667
34	Ca/∑ *A* site	0.985	1.000	1.000	1.000	0.000
35	Si/∑ *T* site	0.001	0.003	0.041	0.041	0.000
36	Dominant *A* site	Ca	Ca	Ca	Ca	Pb
37	Dominant *M* site	□	□	□	□	Fe^{3+}
38	Dominant *Q* site	Be	Be	Be	Be	□
39	Dominant *T* site	P	P	As	As	P
40	Dominant *φ* site	F	OH	OH	F	OH
41	Subgroup	HrdSg	HrdSg	HrdSg	HrdSg	HrdSg
42	Group	HrdG	HrdG	HrdG	HrdG	HrdG
43	Species	Hrd	Hhd	Bgl	Fbgl	Dru

Note: (*apfu*) = Atoms per formula unit. □ = vacancy. Data sources: S1 = Harlow and Hawthorne (2008) S2 = Gorelova et al. (2020); S3, S4, S5 = Handbook of Mineralogy (Anthony et al. 2001–2005). HrdSg = Herderite subgroup; HrdG = Herderite group; Hrd = Herderite, Hhd = Hydroxyl herderite, Bgl = Bergslagite, Fbgl = *Fluorbergslagite*, Dru = Drugmanite. The formulae were recalculated to apfu on the basis of 10 oxygens. The analysis in S4 is the same as in S3 (i.e., bergslagite), but the H_2O (wt. %) content has been intentionally replaced with the F (wt. %) to obtain fluorbergslagite through the program

site, following the dominant-valence rule and dominant occupancy and valence at the *A* and *Q* sites, respectively.

WinGadclas calculates the gadolinite-supergroup mineral analyses (e.g., see rows 1–68 in Tab. 3) and lists the total contents of *A*, *M*, and (*Q*+*T*) sites (apfu), as well as some useful cation/total site ratios (see rows 69–75 in Tab. 3). The determination of dominant constituents by the program at each site (see rows 76–80 in Tab. 3), along with a subgroup, group, and specific species (see rows 81–83 in Tab. 3) based on the current gadolinite-supergroup nomenclature scheme, is provided on the *Calculation Screen* as well as in an output Excel file. The

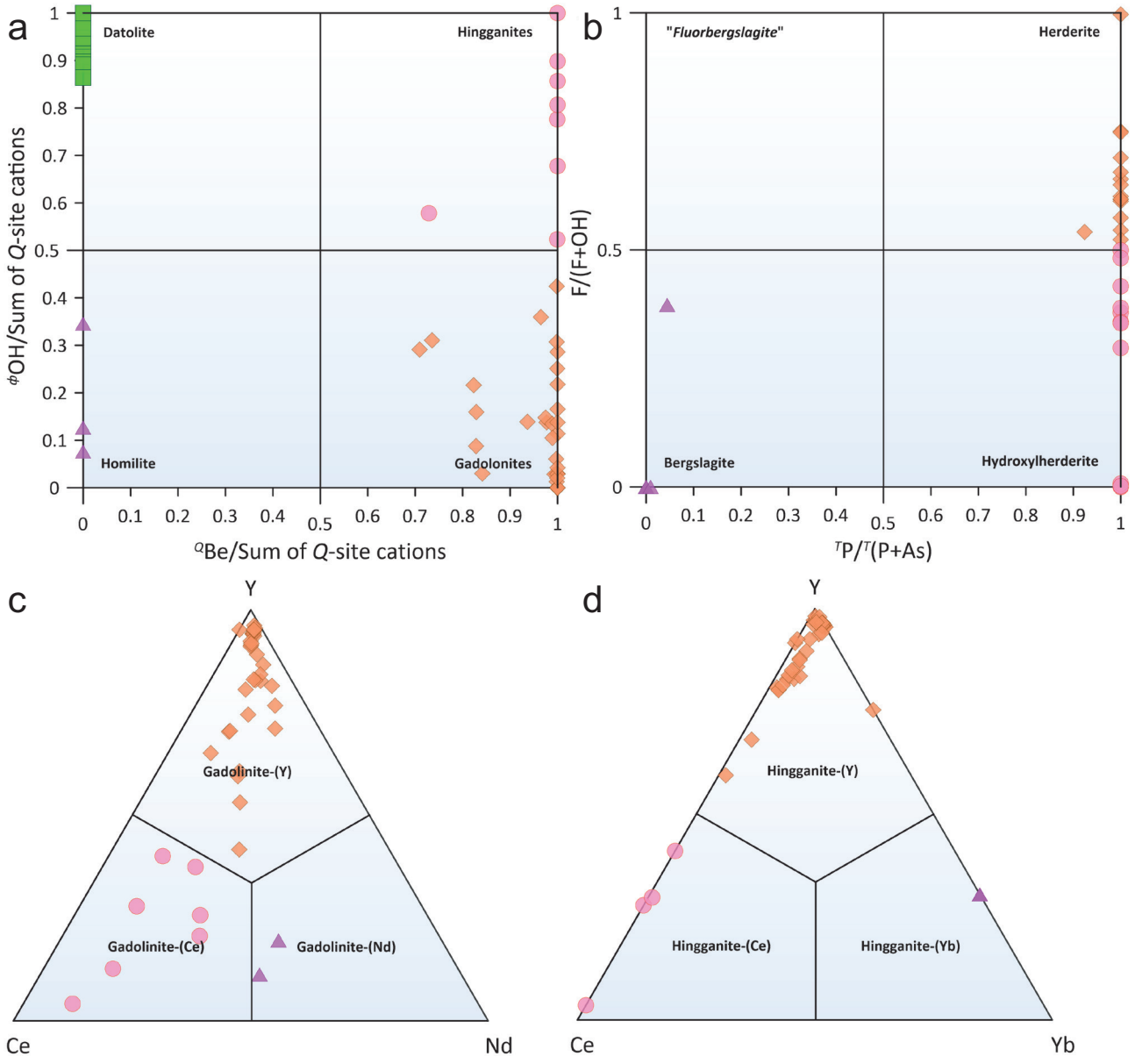

Fig. 2 – Selected plots of the gadolinite-supergroup minerals classification and compositional diagrams from the pull-down menu of *Graph* in the *Calculation Screen* of the WinGadclas program, using the selected mineral analyses from the literature. **a** – Compositional plot of the gadolinite-group minerals in a ^{Q}Be/Sum of *Q*-site cations versus $^{\Phi}$OH/Sum of *Q*-site cations diagram (revised from Gorelova et al. (2021) [filled diamonds from Demartin et al. (1993), Pezzotta et al. (1999), Allaz et al. (2020), Tomašić et al. (2020); filled squares from Demartin et al. (1993), Pezzotta et al. (1999), Tomašić et al. (2020); filled triangles from Gorelova et al. (2024); filled circles from Rinaldi et al. (2010), Kiss et al. (2012), Gorelova et al. (2024)]. **b** – Compositional plot of the herderite-group minerals in a ^{T}P/^{T}(P+As) versus F/(F+OH) diagram (revised from Bačík et al. (2017) [filled diamonds from Huang et al. (2002), Harlow and Hawthorne (2008), Filho et al. (2016), Hien-Dinh et al. (2017); filled circles from Černá et al. (2002), Huang et al. (2002); filled triangles from Brugger and Gieré (1999), Raade et al. (2006)]. **c** – Compositional plot of the gadolinites in a ternary Y–Ce–Nd diagram [filled diamonds from Pezzotta et al. (1999), Allaz et al. (2020), Tomašić et al. (2020), Gorelova et al. (2021); filled circles from Segalstad and Larsen (1978), Lyalina et al. (2019), Allaz et al. (2020); filled triangles from Bačík et al. (2014), Škoda et al. (2018)]. **d** – Compositional plot of the hingganites in a ternary Y–Ce–Yb diagram [filled diamonds from Pezzotta et al. (1999), Pršek et al. (2010), Lyalina et al. (2014, 2019), Chukanov et al. (2017), Gorelova et al. (2020), Majka et al. (2022), Ondrejka et al. (2022, 2023); filled circles from Segalstad and Larsen (1978), Miyawaki et al. (2007), Chakrabarty et al. (2013), Lyalina et al. (2019); filled triangles from Voloshin et al. (1984), Lyalina et al. (2019)].

number of ions is calculated on the basis of 10 oxygen atoms (apfu) in Tabs 3–4. In a case where a chemical composition corresponds to a hitherto unknown species within the gadolinite supergroup (i.e., a new species), WinGadclas warns the user with a "Not classified" statement in columns 119, 120, and 121 of the *Calculation Screen* for subgroup, group, and species, respectively. The program also classifies gadolinite-supergroup species that have not been approved by the IMA (e.g., "Ca-hingganite-(Y)", "OH-gadolinite") but have appeared in

the literature (e.g., Chukanov et al. 2017; Cooper et al. 2019). These mineral species are listed by the program in column 121 of the *Calculation Screen*, as well as in an output Excel file (i.e., `Output.xlsx`), with the necessary explanation under the "Additional Information" title as a statement; for example, "Not approved by the IMA" in column 122. WinGadclas provides options to display binary and ternary classification and compositional diagrams in the *Calculation Screen* by using the Grapher program. Some of these plots, with selected gadolinite-supergroup mineral data from the literature, are shown in Fig. 2. All input and calculated parameters from the *Output* tab of an Excel file (i.e., `Output.xlsx`) are automatically transposed by the *Transpose* tab of the program. This procedure provides the user with the ability to prepare a quick table for presentation as well as publication by using the *Copy–Paste* option.

5. Summary and availability of the program

WinGadclas is a user-friendly program that is specially developed for personal computers running on the Windows operating system to estimate and classify the gadolinite-supergroup minerals using data obtained from both electron-microprobe and wet-chemical analyses. The program processes multiple analytical data sets (up to 200) for each program execution. The current version of WinGadclas recalculates ions, allocates them into the *A*, *M*, *Q*, *T*, and φ sites, and classifies a total of 13 valid species for a given analysis into one of two groups (i.e., gadolinite and herderite) and four subgroups (i.e., datolite, gadolinite, herderite, and drugmanite) using the current IMA-approved nomenclature scheme (Bačík et al. 2017). The program generates two main windows. The first window (i.e., *Start-up/Data Entry Screen*), with several pull-down menus and equivalent shortcuts, enables users to edit a given gadolinite-supergroup mineral analysis based on chemistry (wt. %). By clicking the *Calculate* icon (i.e., ∑) in the *Data Entry Screen*, all input and estimated parameters by WinGadclas are displayed in the second window (i.e., *Calculation Screen*). The program reports the output in a tabulated form with columns numbered from 1 to 121 in the *Calculation Screen* window, as well as in an output Excel file. These columns include the gadolinite-supergroup compositions (wt. %), recalculated cation and anion values (apfu), total contents of ions (apfu) allocated to the sites, along with some useful ratios, dominant ions at the sites (i.e., *A*, *M*, *Q*, *T*, and φ), as well as groups, subgroups, and species. The results in the *Calculation Screen* can be exported to a Microsoft® Excel file (i.e., `Output.xlsx`), by clicking the *Send Results to Excel File (Output.xlsx)* icon or selecting the *Send Results to Excel File (Output.xlsx)* option from the pull-down menu of *Excel*. This file is then opened by Excel by clicking the *Open and Edit Excel File (Output.xlsx)* icon or selecting the *Open Excel File (Output.xlsx)* option from the pull-down menu of *Excel*.

WinGadclas is a compiled program that consists of a self-extracting setup file containing all the necessary support files (i.e., "`dll`" and "`ocx`") for the 32-bit system. By clicking the setup file, the program and its associated files (i.e., support files, help file, data files with the extensions "`.gad`", "`.xls`", "`.xlsx`" and plot files with the extension "`.grf`" are installed into the personal computer (i.e., the directory of `C:\Program Files\WinGadclas or C:\Program Files (x86)\WinGadclas`) on Windows 7 or subsequent operating systems. An installation of the program on a personal computer with a 64-bit operating system may require the "`msflexgrd`" adjustment (see explanations in the Electronic Supplementary Material, ESM 1). The self-extracting setup file (i.e., the WinGadclas `setup.exe` file) is approximately 9 MB and can be obtained from the journal's server as a Electronic Supplementary Material (ESM 2).

Acknowledgements. I am grateful to Daniel Atencio and Fernando Cámara for their valuable contributions and suggestions on an earlier draft. I wish also thank Peter Bačík and Petr Gadas for their constructive comments, which improved the overall quality and clarity of the manuscript. I also express my thanks to Vojtěch Janoušek for his editorial handling and valuable contributions.

Electronic supplementary material. The installation of the WinGadclas setup.EXE file, along with the corresponding instructions, can be accessed online at the Journal's website. (*http://dx.doi.org/10.3190/jgeosci.404*).

References

Allaz JM, Smyth Jr, Henry RE, Stern CR, Persson P, Ma JJ, Raschke MB (2020) Beryllium–silicon disorder and rare earth crystal chemistry in gadolinite from the white cloud pegmatite, Colorado, USA. Canad Mineral 58: 829–845

Anthony JW, Bideaux RA, Bladh KW, Nichols MC (2001–2005) Handbook of Mineralogy. Mineralogical Society of America, Chantilly, Virginia 20151-1110, USA. Accessed on April 24, 2025, at http://www.handbookofmineralogy.org

Atencio D (2023) Minasgeraisite-(Y) discredited as an ordered intermediate between datolite and hingganite-(Y). Mineral Mag 87: 738–740

Bačík P, Fridrichová J, Uher P, Pršek J, Ondrejka M (2014) Crystal chemistry of gadolinite–datolite group minerals. Canad Mineral 52: 625–642

Bačík P, Miyawaki R, Atencio D, Cámara F, Fridrichová J (2017) Nomenclature of the gadolinite supergroup. Eur J Mineral 29: 1067–1082

Brugger J, gieré R (1999) As, Sb, Be and Ce enrichment in minerals from a metamorphosed Fe–Mn deposit, Val Ferrera, eastern Swiss Alps. Canad Mineral 37: 37–52

Cámara F, Oberti R, Ottolini L, Della Ventura G, Bellatreccia F (2008) The crystal chemistry of Li in gadolinite. Am Mineral 93: 996–1004

Černá I, Černý P, Selway JB, Chapman R (2002) Paragenesis and origin of secondary beryllophosphates: beryllonite and hydroxylherderite from the Bep granitic pegmatite, southeastern Manitoba, Canada. Canad Mineral 40: 1339–1345

Chakrabarty A, Mitchell RH, Ren M, Sen AK, Pruseth KL (2013) Rinkite, cerianite-(Ce), and hingganite-(Ce) in syenite gneisses from the Sushina Hill Complex, India: occurrence, compositional data and petrogenetic significance. Mineral Mag 77: 3137–3153

Chukanov NV, Aksenov SM, Rastsvetaeva RK, Kristiansen R, Pekov IV, Belakovskiy DI, Van KV, Bychkovah YV, Britvin SN (2017) Crystal structure of the OH-dominant gadolinite-(Y) analogue $(Y,Ca)_2(Fe,□)Be_2Si_2O_8(OH,O)_2$ from Heftetjern pegmatite, Norway. Acta Cryst B73: 899–906

Cooper MA, Hawthorne FC, Miyawaki R, Kristiansen R (2019) Cation order in the crystal structure of 'Ca-Hingganite-(Y)'. Canad Mineral 57: 371–382

Demartin F, Pilati T, Diella V, Gentile P, Gramaccioli CM (1993) A crystal–chemical investigation of Alpine gadolinite. Canad Mineral 30: 127–136

Filho LADM, De Sá Carneiro Chaves ML, Dias CH, Atencio D (2016) Recent mineral discoveries in the Coronel Murta, Taquaral, and Medina pegmatite field, northeastern Minas Gerais, Brazil. Rem – Int Eng J 69: 301–307

Foit FF, Phillips MW, Gibb GV (1973) A refinement of the crystal structure of datolite, $CaBSiO_4(OH)$. Am Mineral 58: 909–914

Gorelova L, Vereshchagin O, Cuchet S, Shilovskikh V, Pankin D (2020) Low-temperature crystal chemistry of hingganite-(Y), from the Wanni Glacier, Switzerland. Minerals 10, 322

Gorelova LA, Panikorovskii TL, Pautov LA, Vereshchagin OS, Krzhizhanovskaya MG, Spiridonova Dar'ya V (2021) Temperature-versus compositional-induced structural deformations of gadolinite group minerals with various Be/B ratio. J Solid State Chem 299: 122187

Gorelova LA, Vereshchagin OS, Shagova AK, Krzhizhanovskaya MG, Pankin DV, Bocharov VN, Kasatkin AV, Pekov IV (2024) Topotactic transformation of gadolinite- to melilite-type structure revisited. J Am Ceram Soc 107: 3534–3549

Harlow GE, Hawthorne FC (2008) Herderite from Mogok, Myanmar, and comparison with hydroxylherderite from Ehrenfriedersdorf, Germany. Am Mineral 93: 1545–1549

Hatert F, Burke EAJ (2008) The IMA–CNMNC dominant-constituent rule revisited and extended. Canad Mineral 46: 717–728

Hawthorne FC, Gagné OC (2024) New ion radii for oxides and oxysalts, fluorides, chlorides and nitrides. Acta Cryst: B80, 326–339

Hien-Dinh TT, Dao DA, Tran T, Wahl M, Stein E, Gieré R (2017) Lithium-rich albite–topaz–lepidolite granite from Central Vietnam: a mineralogical and geochemical characterization. Eur J Mineral 29: 1–18

Huang XL, Wang RC, Chen XM, Hu H, Liu CS (2002) Vertical variations in the mineralogy of the Yichun topaz–lepidolite granite, Jiangxi province, southern China. Canad Mineral 40: 47–68

Ito J, Hafner SS (1974) Synthesis and study of gadolinites. Am Mineral 59: 700–708

Janoušek V, Farrow CM, Erban V (2024) GCDkit.Mineral: a customizable, platform-independent R-language environment for recalculation, plotting, and classification of electron probe microanalyses of common rock-forming minerals. Am Mineral 109: 1598–1607

King GSD, Sengier-Roberts L (1988) Drugmanite, $Pb_2(Fe_{0.78}Al_{0.22})H(PO_4)_2(OH)_2$: its crystal structure and place in the datolite group. Bull Minéral 111: 431–437

Kiss G, Molnár F, Zaccarini F (2012) Fluid inclusion studies in datolite of low grade metamorphic origin from a Jurassic pillow basalt series in northeastern Hungary. Cent Eur J Geosci 4: 261–274

Levinson AA (1966) A system of nomenclature for rare-earth minerals. Am Mineral 51: 152–158

Lyalina LM, Selivanova EA, Savchenko YEE, Zozulya DR, Kadyrova GI (2014) Minerals of the gadolinite-(Y)–hingganite-(Y) series in the alkali granite pegmatites of the Kola Peninsula. Geol Ore Depos 56: 675–684

Lyalina LM, Selivanova EA, Zozulya DR, Ivanyuk GY (2019) Beryllium mineralogy of the Kola Peninsula, Russia – a review. Minerals 9: 12

Majka J, Włodek A, Jonsson E, Högdahl K (2022) Contrasting coronas: microscale fluid variation deduced from monazite breakdown products in altered metavolcanic rocks associated with the Grängesberg apatite–iron oxide ore, Bergslagen, Sweden. GFF 144: 89–96

Miyawaki R, Matsubara S, Yokoyama K, Okamoto A (2007) Hingganite(Ce) and hingganite-(Y) from Tahara, Hirukawa-mura, Gifu Prefecture, Japan: the description on a new mineral species of the Ce-analogue of hingganite-(Y) with a refinement of the crystal structure of hingganite-(Y). J Miner Petrol Sci 102: 1–7

Ondrejka M, Molnárová A, Putiš M, Bačík P, Uher P, Voleková B, Milovská S, Mikuš T, Pukančík L (2022)

Hellandite-(Y)–hingganite-(Y)–fluorapatite retrograde coronae: a novel type of fluid-induced dissolution–reprecipitation breakdown of xenotime-(Y) in the metagranites of Fabova Hoľa, Western Carpathians, Slovakia. Mineral Mag 86: 586–605

Ondrejka M, Uher P, Ferenc Š, Milovská S, Mikuš T, Molnárová A, Škoda R, Kopáčik R, Bačík P (2023) Gadolinium-dominant monazite and xenotime: selective hydrothermal enrichment of middle REE during low-temperature alteration of uraninite, brannerite, and fluorapatite (the Zimná Voda REE–U–Au quartz vein, Western Carpathians, Slovakia). Am Mineral 108: 754–768

Paulmann C, Zietlow P, McCammon C, Salje EKH, Bismayer U (2019) Annealing of metamict gadolinite-(Y): X-ray diffraction, Raman, IR, and Mössbauer spectroscopy. Z Kristallogr 234: 587–593

Pezzotta F, Diella V, Guastoni A (1999) Chemical and paragenetic data on gadolinite-group minerals from Baveno and Cuasso al Monte, southern Alps, Italy. Am Mineral 84: 782–789

Pršek J, Ondrejka M, Bačík P, Budzyń B, Uher P (2010) Metamorphic–hydrothermal REE minerals in the Bacúch magnetite deposit, western Carpathians, Slovakia: (Sr,S)-rich monazite-(Ce) and Nd-dominant hingganite. Canad Mineral 48: 81–94

Raade G, Kolitsch U, Husdal TA (2006) Si-rich bergslagite from a granitic pegmatite at Tennvatn, north Norway. GFF 128: 65–68

Rinaldi R, Gatta GD, Angel RJ (2010) Crystal chemistry and low-temperature behavior of datolite: a single-crystal X-ray diffraction study. Am Mineral 95: 1413–1421

Segalstad TV, Larsen AO (1978) Gadolinite-(Ce) from Skien, southern Oslo region, Norway. Am Mineral 63: 188–195

Škoda R, Plášil J, Čopjaková R, Novák M, Jonsson E, Galiová MV, Holtstam D (2018) Gadolinite-(Nd), a new member of the gadolinite supergroup from Fe–REE deposits of Bastnäs-type, Sweden. Mineral Mag 82: 133–145

Tomašić N, Škoda R, Bermanec V, Šoufek M (2020) Crystal chemistry and microfeatures of gadolinite imprinted by pegmatite formation and alteration evolution. Am Mineral 105: 1647–1655

Vereshchagin OS, Gorelova LA, Anastasia K, Shagova AK, Kasatkin AV, Škoda R, Bocharov VN, Vlasenko NS, Galiová MV (2023) Re-investigation of 'minasgeraisite-(Y)' from the Jaguaraçu pegmatite, Brazil and high-temperature crystal chemistry of gadolinite-supergroup minerals. Mineral Mag 87: 470–479

Voloshin AV, Pakhomovskii YAA, Men'shikov YUP, Povarennykh AS, Matvinenko EN, Yakubovich OV (1984) Hingganite-(Yb), a new mineral from amazonite pegmatite of the Kola Peninsula. Int Geol Rev 26: 60–63

Yavuz F (1999) A revised program for microprobe-derived amphibole analyses using the IMA rules. Comput Geosci 25: 909–927

Yavuz F (2003) Evaluating micas in petrologic and metallogenic aspect: I – definitions and structure of the computer program MICA^{+}. Comput Geosci 29: 1203–1213

Yavuz F (2013) WinPyrox: a Windows program for pyroxene calculation classification and thermobarometry. Am Mineral 98: 1338–1359

Yavuz F (2021) WinMIgob: A Windows program for magnetite–ilmenite geothermometer and oxygen barometer. J Geosci 66: 51–70

Yavuz F (2024a) WinTtrclas, a Windows program for tetrahedrite-group minerals. Period Mineral 93: 127–145

Yavuz F (2024b) WinClbclas, a Windows program for columbite-supergroup minerals. Mineral Mag 88: 439–450

Yavuz F (2025a) WinCrtclas, a Windows program for cerite-supergroup minerals. Period Mineral 94: 37–51

Yavuz F (2025b) WinHolclas, a Windows program for hollandite-supergroup minerals. Period Mineral 94: 281–292

Yavuz F, Yavuz EV (2022) A Windows program for feldspar group thermometers and hygrometers. Period Mineral 91: 63–87

Yavuz F, Yavuz V (2023a) WinApclas, A Windows program for apatite supergroup minerals. Period Mineral 92: 307–333

Yavuz F, Yavuz V (2023b) WinSpingc, a Windows program for spinel supergroup minerals. J Geosci 68: 95–110

Yavuz F, Yavuz V (2024) WinPclclas, A Windows program for pyrochlore supergroup minerals. CJMP 2: 165–185

Yavuz F, Yildirim DK (2018) A Windows program for calculation and classification of epidote-supergroup minerals. Period Mineral 872: 269–285

Yavuz F, Yildirim DK (2020) WinGrt, a Windows program for garnet supergroup minerals. J Geosci 65: 71–95

Yavuz F, Karakaya N, Yildirim DK, Karakaya MÇ, Kumral M (2014) A Windows program for calculation and classification of tourmaline-supergroup (IMA-2011). Comput Geosci 63: 70–87

Yavuz F, Kumral M, Karakaya N, Karakaya MÇ, Yildirim DK (2015) A Windows program for chlorite calculation and classification. Comput Geosci 81: 101–113